*buildings*

MDPI

*Article*

# Evaluation of Shear Connection Methods for Bamboo–Concrete Composite Structures

**José Henriques [1,*] and Jemal Jibril [2]**

[1] Construction Engineering Research Group, Faculty of Engineering Technology, Hasselt University, B3590 Diepenbeek, Belgium
[2] Faculty of Civil and Environmental Engineering, Jimma Institute of Technology, Jimma University, Jimma P.O. Box 378, Ethiopia; jibril.mohammed@ju.edu.et
* Correspondence: jose.gouveiahenriques@uhasselt.be; Tel.: +32-11-29-21-60

**Abstract**

The construction sector faces growing pressure to reduce its environmental impact, particularly in regions with limited access to conventional materials and urgent housing needs. Bamboo, a fast-growing and renewable resource with favorable mechanical properties, offers a sustainable alternative for structural applications. This study aims to enhance the efficiency of bamboo–concrete composites by investigating shear connection methods for composite floor systems. Different connection configurations were examined: (i) notch-type, (ii) dowel-type, and (iii) combined systems. Symmetric push-out tests were conducted to evaluate the load transfer mechanisms between bamboo logs and concrete layers. The mechanical behavior of each configuration was characterized through load–slip responses, failure modes, stiffness, strength, and deformation capacity. The results show that notch-type connections with longer grooves provided the highest stiffness and strength. In contrast, dowel-type connections exhibited superior ductility but lower stiffness and strength. The combined configuration delivered a balanced performance, integrating favorable aspects of both systems. A predictive model for each connection type was developed and validated against the experimental data, demonstrating satisfactory accuracy and reliable prediction of failure modes. These findings highlight the potential of optimized shear connections to advance sustainable bamboo–concrete composite construction, while also revealing the significant influence of bamboo's natural variability, such as differences in diameter, node geometry, straightness, and material properties, on structural performance.

**Keywords:** bamboo-concrete composite; shear connection; notch; dowel-type; push-out tests



Academic Editor: Antonio Formisano

Received: 15 October 2025
Revised: 7 November 2025
Accepted: 19 November 2025
Published: 28 November 2025

**Citation:** Henriques, J.; Jibril, J. Evaluation of Shear Connection Methods for Bamboo–Concrete Composite Structures. *Buildings* **2025**, *15*, 4320. https://doi.org/10.3390/buildings15234320



## 1. Introduction

The construction sector is responsible for approximately 50% of global material consumption, 33% of total solid waste in Europe, and 36% of carbon emissions [1]. At the same time, urbanization is expected to increase, with 60% of the world's population projected to live in cities by 2030 [2]. This dual pressure—rising demand for housing and the need to reduce environmental impacts—highlights the urgency of transitioning toward more sustainable construction practices. The sector must adopt strategies to extend the life of existing structures, integrate bio-based materials, manage waste, and lower emissions. These challenges are particularly acute in developing countries, where access to conventional materials is limited and housing deficits remain significant. In Ethiopia, for instance, more than 70% of the population lives in vulnerable housing conditions [3]. The use of

locally available resources such as bamboo, complemented with agricultural and industrial by-products, offers a cost-effective and environmentally responsible opportunity.

Bamboo combines rapid renewability [4], high strength-to-weight ratio [5], and suitability for structural applications [6]. Ethiopia is especially rich in bamboo resources, hosting both Oldeania alpina and Oxytenanthera abyssinica, and accounting for 67% of Africa's and 7% of the world's bamboo reserves [7,8]. Despite this abundance, the structural potential of bamboo remains largely underexploited in Africa [8].

Composite approaches provide an effective way to enhance material performance by exploiting synergies. Two primary methods can be identified for combining bamboo with concrete: (i) Material-level integration, in which bamboo fibers are incorporated into the concrete matrix to produce bamboo fiber-reinforced concrete; and (ii) Member-level combination, which involves either substituting bamboo for conventional steel reinforcement bars or forming a composite structural member where bamboo is combined with a concrete top layer. While bamboo fiber-reinforced concrete has been extensively investigated in previous studies [9], it falls outside the scope of this research. The present study focuses instead on member-level combinations of bamboo and concrete.

Similar to advances in timber–concrete systems [10,11], combining bamboo with concrete offers the potential to deliver more competitive and resilient structural solutions. Previous research has considered bamboo as reinforcement in concrete [12,13] and as permanent formwork in bamboo–concrete floors [12,14]. In the latter, first explored by Ghavami [12], bamboo segments formed permanent formwork beneath a concrete layer. However, adhesion and knot interlock proved insufficient for adequate load transfer, leading to limited shear resistance. Modified approaches—such as partial opening of bamboo segments to improve interlock [12] or reinforcement with steel [14]—improved flexural strength, but the shear transfer mechanisms remained only indirectly addressed. The present investigation aims to advance the understanding of composite floor systems that combine bamboo logs with a concrete top layer by exploring the connection methods between these materials.

Overall, the literature on bamboo–concrete composites remains limited, with most studies focused on global bending behavior rather than the performance of shear connections, which are critical for composite action. To address this gap, the present study investigates the load–slip behavior of shear connections in bamboo–concrete composite floors, not yet covered by previous studies. Four connection configurations were developed, inspired by existing timber–concrete composite solutions [12,15–17], and evaluated through experimental push-out tests. The findings, while contributing with novel experimental data, provide insight into stiffness, strength, ductility, and failure mechanisms, while an analytical predictive model—adapted from established design standards [18]—was proposed and validated against experimental results. This study advances the understanding of bamboo–concrete shear connection, targeting a composite action, and contributes to the development of sustainable structural systems for affordable housing.

## 2. Materials and Methods

### *2.1. Proposed Shear Connections for Bamboo-Concrete Composite*

In structural engineering, the term composite is not always used consistently and is sometimes confused with hybrid. In this study, a composite beam or floor member refers to a structural system in which two or more materials act synergistically, resulting in overall stiffness and strength greater than the simple sum of the individual components. For bending members incorporating shear connections, as investigated in this research, the strain distribution within each material is interdependent and directly influenced by the mechanical performance of the shear connection that enables composite action. The

degree of interaction between materials [19] can be classified as follows: (i) *Full interaction*: Negligible slip occurs between materials, and the strain distribution is continuous throughout the composite cross-section (Figure 1c). (ii) *Partial interaction*: Limited slip develops at the interface, resulting in a nonlinear strain distribution across the composite section. Within each material, strains remain approximately linear but are influenced by interfacial slip (Figure 1b). (iii) *No interaction*: Significant slip occurs between materials, leading to independent distribution of strains and the absence of composite action (Figure 1a).

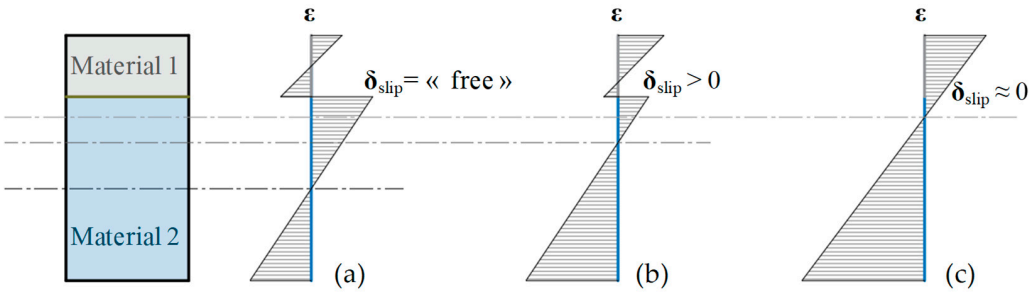


**Figure 1.** Classification defining the level of interaction in composite members. (**a**) No Interaction. (**b**) Partial Interaction. (**c**) Complete Interaction.

The structural efficiency of a composite member increases with the level of interaction, from no to full interaction. Since this efficiency depends on the mechanical behavior of the shear connection, the latter plays a fundamental role in composite systems. In a shear connection, three mechanical properties are particularly relevant: (i) *Shear stiffness* ($k_i$): Determines the magnitude of slip, higher stiffness results in smaller slip and stronger composite action; (ii) *Shear strength* ($F_v$): Defines the maximum shear load transferable between materials; (iii) *Ductility* ($D$): Represents the connection's capacity to sustain shear load under increasing slip, allowing redistribution of forces among adjacent connectors without premature failure. Typically, ductility is defined by a 20% reduction in load capacity after the peak shear load [20]. Although these properties govern composite action efficiency, in members subjected to bending, shear connectors also experience a separation force normal to the slip plane. Despite being relatively small, this effect should not be neglected during connection design. The bamboo–concrete interface introduces additional challenges: (i) bamboo's limited shear strength and brittle behavior along the grain; (ii) difficulties in anchoring fasteners due to bamboo's hollow cross-section and susceptibility to cracking; (iii) concrete's low tensile and shear strength in the absence of reinforcement.

Considering these challenges, various shear connection configurations for bamboo–concrete composite beams and floors were conceived and tested in this research (Table 1). Four configurations were developed and experimentally evaluated, based on two main connection principles: notch-type (N) and dowel-type (D) systems. The notch-type connection is inspired by timber–concrete composite (TCC) solutions [21,22], where a groove or block in the timber provides mechanical interlock with concrete to resist slip. In bamboo–concrete members, an incision is made in the bamboo culm to allow concrete to penetrate during casting, forming a similar interlocking mechanism. The dowel-type connection, also adapted from TCC systems [23,24], involves drilling a hole through the bamboo cross-section to install a steel reinforcement bar (dowel). The hole diameter is slightly smaller than the rebar's nominal diameter to ensure a tight fit, and installation is carried out carefully with a hammer to prevent bamboo damage. The dowel extends across the bamboo culm to engage both "walls" of the hollow section, mobilizing two contact zones and developing a binary resistance mechanism that restricts dowel rotation under shear loading.

**Table 1.** Developed shear connection configurations for bamboo-concrete composite members.

| ID | Description | Schematic Illustration |
|---|---|---|
| SN | An opening is cut into the bamboo culm to a depth of about three-quarters of its diameter, positioned midway between nodes, with a length equal to roughly one-third of the internodal distance (Small, S). | 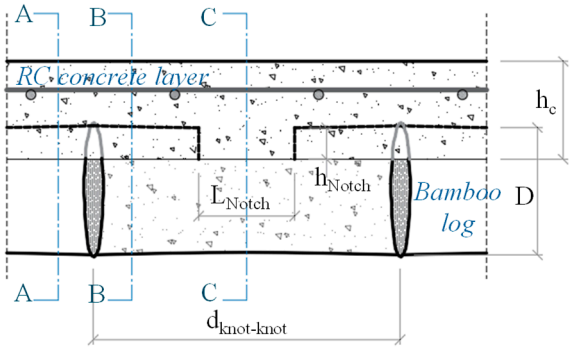  |
| LN | An opening is cut into the bamboo culm to a depth of about three-quarters of its diameter, positioned midway between nodes, with a length equal to roughly two-thirds of the internodal distance (Large, L). | |
| D | A ribbed steel reinforcement bar passes through the entire bamboo culm, extending beyond the bamboo culm into the concrete side to mobilize dowel action (embedment length). | 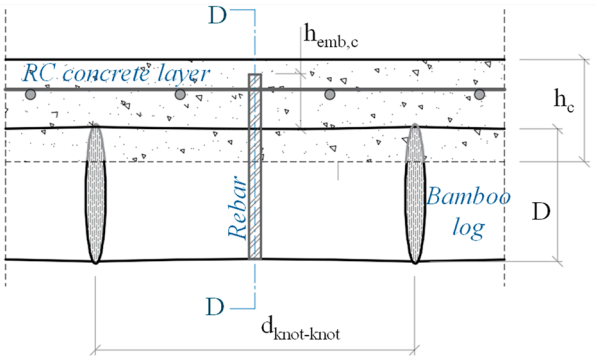  |
| SND | This configuration combines a small notch (S) with a dowel (D) in the same segment. In full-scale floor applications, the notch and dowel could be installed in separate segments, but this arrangement was not tested due to height limitations in the experimental setup. | 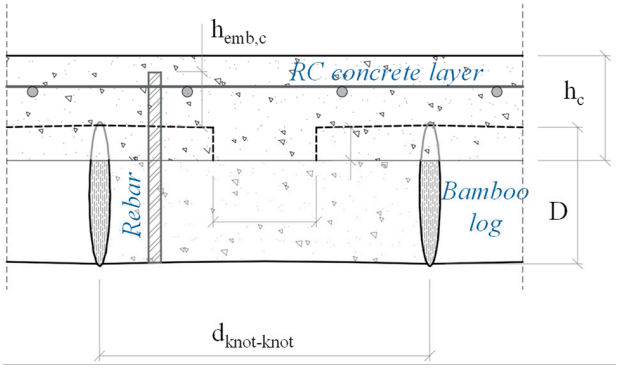  |
| | | 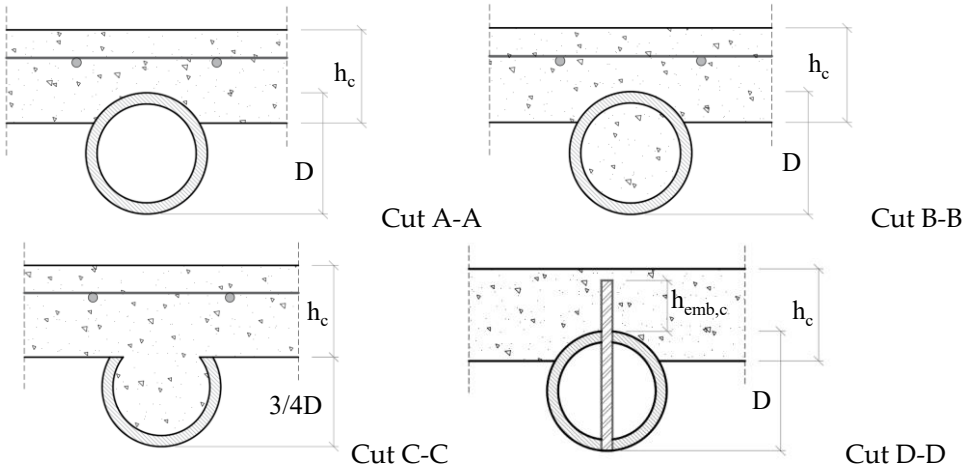  |

### *2.2. Experimental Program*

#### 2.2.1. Test Specimens and Materials

The four configurations described in Section 2.1 were investigated experimentally. Each test specimen consisted of two bamboo logs connected by a concrete layer placed between them. The specimen geometry and testing variables are summarized in Table 2 and illustrated in Figure 2. A total of twelve specimens were produced, with three replicas per configuration. The bamboo log diameters (D) and concrete layer thickness (70 mm) were selected based on the largest available bamboo diameter and common practice in research on TCC floors [25], respectively. The total specimen length was constrained by the test setup (described in the next section), and a deliberate misalignment between the bottom edges was introduced to allow slip during push-out tests. Specimen preparation was challenging due to bamboo irregularities, including knots and variations in diameter along the length (Figure 3a), as well as pre-existing cracks from natural or uncontrolled drying (Figure 3b). Although bamboo selection was performed, eliminating all imperfections was neither possible nor desired, since such irregularities are inevitable in real applications. Consequently, while the tests were designed for symmetric specimens (Figure 2), potential eccentricities must be considered. Additionally, concrete was cast through the side of the formwork (Figure 3a), which made it challenging to achieve complete filling of the bamboo logs due to limited access for the vibrator tip (internal vibration method used). The final test specimens are shown in Figure 3c.

**Table 2.** Summary of the testing program.

| Test Specimen ID | Connection Method | | Number of Replicas |
|---|---|---|---|
| | Notch | Dowel | |
| SN-i | $L_{Notch} \approx 150$ mm<br>$h_{Notch} \approx 32.5$ mm | | 3 |
| LN-i | $L_{Notch} \approx 300$ mm<br>$h_{Notch} \approx 32.5$ mm | | 3 |
| D-i | | $d_R = 12$ mm<br>$L_R = D + 50$ mm<br>$h_{emb,C} =$ Min 50 mm | 3 |
| SND-i | $L_{Notch} \approx 150$ mm<br>$h_{Notch} \approx 32.5$ mm | $d_R = 12$ mm<br>$L_R = D + 50$ mm<br>$h_{emb,C} =$ Min 50 mm | 3 |

i = 1 to 3; D is the bamboo log diameter which is variable.

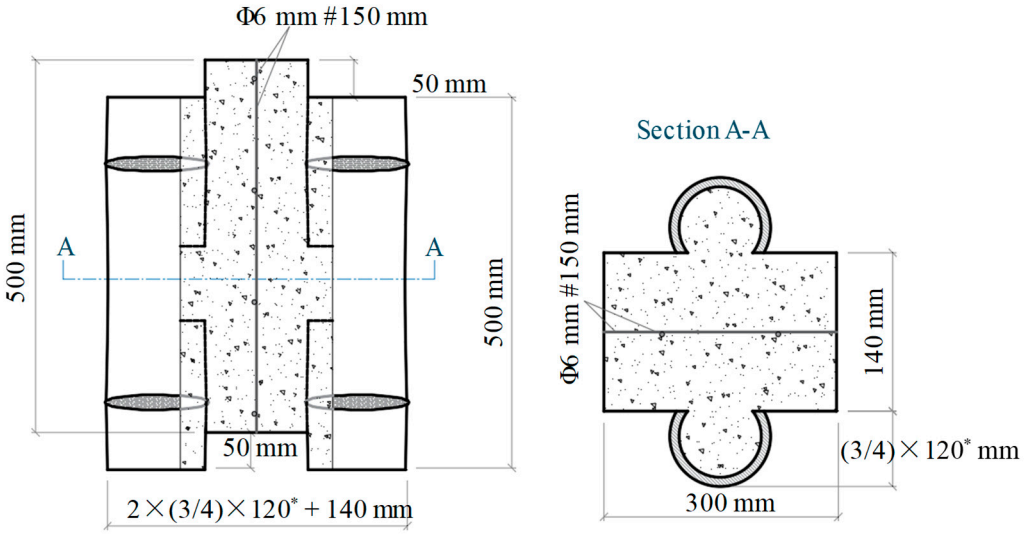


**Figure 2.** Geometry of the test specimens (* 120 mm is the average bamboo log diameter, D).

(**a**) (**b**) (**c**)

**Figure 3.** Test specimens. (**a**) Test specimen in preparation for casting (formwork detail). (**b**) Test specimen with cracked bamboo log. (**c**) Test specimen before testing.

The materials used in the test specimens included: (i) C20/25 concrete, (ii) *Guadua Angustifolia* bamboo, and (iii) S500 ribbed steel bars. Compression tests were performed on both the concrete and bamboo to determine their actual mechanical properties, as presented in Section 3. Additionally, an S500 steel mesh (#150 × 150 Φ5) was embedded within the concrete layer.

#### 2.2.2. Test Setup, Loading Procedure and Monitoring

The experimental program consisted of classical symmetric push-out tests under short-term loading, as illustrated in Figure 4. Given that no standard is specifies the testing procedure for bamboo-concrete push-out tests, the recommendations given in the EN 26891 [26] were used as general guidance. Due to some limitations during the execution, the loading-unloading-reloading cycle was not realized. Tests were performed using a 250 kN tensile testing machine (*MPM Dartec Mod 250* kN). A hydraulic jack applied an upward load to the bamboo logs, which was transferred to the concrete layer through the shear connection.

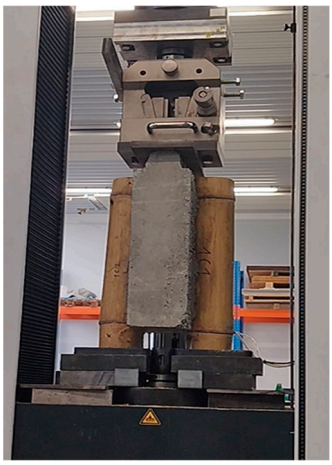

**Figure 4.** Test setup.

The load was initially applied imposing a constant deformation rate of 0.5 mm/min until the specimen reached its maximum load capacity. To capture the post-peak load–deformation behavior, in order to limit the test duration, the deformation rate was then increased until fracture occurred or the gap between the concrete and bamboo at the

bottom was closed. Load and displacement were monitored using the machine's load cell and integrated displacement gauges. The displacement gauges measured the stroke of the hydraulic jack, reflecting the total deformation of the specimen under load. Shear connection slip was obtained by subtracting the deformations of the bamboo and concrete during post-processing.

### *2.3. Analytical Approach*

Research on bamboo–concrete composite systems remain limited. Consequently, design methodologies capable of predicting both local load-transfer mechanisms—such as the shear connections investigated in this study—and the global bending behavior of composite floors and beams are still lacking. In contrast, the combination of concrete (or reinforced concrete) with steel or timber has been extensively studied, leading to well-established design approaches that have been incorporated into standards and guidelines over several decades [18,27,28]. Regarding the mechanical behavior of shear connections, as described above, the predictive models developed for timber–concrete composite beams [18] appear to be the most appropriate for adaptation. The proposed extension of these models to the bamboo–concrete shear connections investigated herein is presented below. Later, the accuracy of the proposed models is assessed and discussed.

#### 2.3.1. Notch Connection (N)

In the investigated notched-type shear connections, the load-carrying capacity may be governed by four possible failure mechanisms, as described below and illustrated in Figure 5:

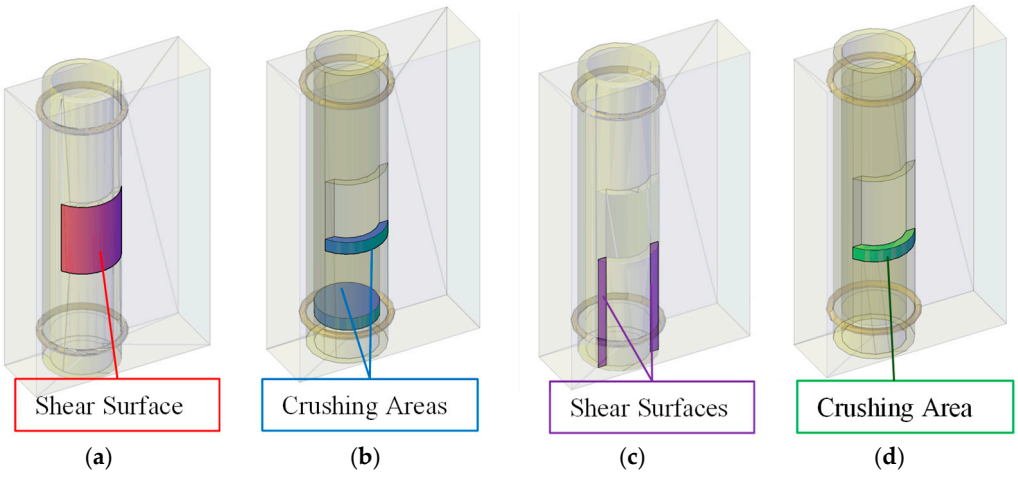


**Figure 5.** Possible modes of failure in bamboo-concrete notch shear connections. (**a**) Concrete shear failure. (**b**) Concrete crushing. (**c**) Bamboo shear failure. (**d**) Bamboo crushing.

a. Shear failure of concrete: occurs when the shear resistance of the concrete at the interface is reached (Figure 5a);

b. Crushing of concrete: develops when the compressive strength of the concrete in the bamboo–wall contact zone is attained (Figure 5b);

c. Shear failure of bamboo: arises when the shear resistance of the bamboo wall is exceeded (Figure 5c);

d. Crushing of bamboo: takes place when the compressive strength along the bamboo fibers is reached (Figure 5d).

The load-carrying capacity corresponding to each of the described failure mechanisms is derived from the design equations specified in CEN/TS 19103 [18], adapted here for the bamboo–concrete shear connections investigated in this study. Table 3 summarizes the

proposed predictive equations for each possible failure mode. Accordingly, the overall resistance of the shear connection is governed by the weakest failure mode, as indicated in Table 3.

**Table 3.** Predictive design equations for notch shear connections in bamboo-concrete composite solutions.

| Failure Mode | Proposed Equation | |
|---|---|---|
| (a) Shear failure of concrete | $F_{R,a} = f_{v,c} s_n l_n$ | (1) |
| (b) Crushing of concrete | $F_{R,b} = f_{c,c} s_n t_B + f_{c,c} \frac{\pi}{4} d_{i,B}^2$ | (2) |
| (c) Shear of bamboo | $F_{R,c} = k_{cr} f_{v,B} t_B 2 l_B$ | (3) |
| (d) Crushing of bamboo | $F_{R,d} = f_{c,B} s_n t_B$ | (4) |
| Shear connection resistance | Min ($F_{R,a}$; $F_{R,b}$; $F_{R,c}$; $F_{R,d}$) | (5) |

Where: $f_{v,c}$ is the shear strength of the concrete, $s_n$ is arc length of section removed from the bamboo log, $l_n$ is the length of removed section through which the concrete can enter the bamboo log and where the shear line in the concrete will be developed, $f_{c,c}$ is the concrete compressive strength, $t_B$ is the wall thickness of the bamboo log in contact with the concrete, $d_{i,B}$ is the inner diameter of the bamboo log which will be infill with concrete, $k_{cr}$ is cracked factor for bamboo (assumed equal 1 at this stage), $f_{v,B}$ is the shear strength of bamboo along fibers; $l_B$ is the length of the shear line in the bamboo log; $f_{c,B}$ is the bamboo compressive strength in fiber direction.

In the investigated connections, the critical shear stresses in the concrete (illustrated in Figure 5a) develop in the notch zone at the concrete–bamboo interface. Since no reinforcement is provided to enhance the shear capacity of the connection, the shear strength ($f_{v,c}$) is determined differently from the approach prescribed in CEN/TS 19103 [18], which refers to EN 1992-1-1 [29] for reinforced concrete. Instead, the shear strength is evaluated using the Mohr–Coulomb failure criterion, as proposed in [30], and is expressed by Equations (6) and (7) for confined and cracked concrete, respectively.

$$f_{v,c} = \frac{f_{c,c}}{4} \quad (6)$$

$$f_{v,c} = \frac{f_{c,c}}{6} \quad (7)$$

2.3.2. Dowel Connection (D)

In dowel-type connections, the following local failure modes may occur: (i) Embedment strength of the bamboo ($f_{h,B}$) mobilized by local compressive stresses in the bearing area between the bamboo and the steel dowel; (ii) Plastic hinge formation in the steel dowel under bending ($M_{y,k}$); (iii) Local compression of the concrete in bearing with the dowel, equivalent to the embedment strength in bamboo.

The global load-transfer behavior of dowel-type connections is characterized by the possible mobilization of these local mechanisms, either individually or in combination, as described in the model proposed by Johansen [31] for timber structures, later adopted as the European Yield Model (EYM) [32]. These models form the basis of the design provisions in CEN/TS 19103 [18], EN 1995-1-1 [33], and EN 1995-2 [28] for dowel-type connections. In these standards, the load-bearing capacity may include the contribution of the so-called rope effect, which represents the withdrawal resistance mobilized when dowel rotation occurs, with or without plastic hinges. However, because the withdrawal capacity of bamboo is negligible, due to its limited anchorage potential, the rope effect is not considered in this study.

Accordingly, for the investigated connections, two global failure modes (Figure 6) are analyzed:

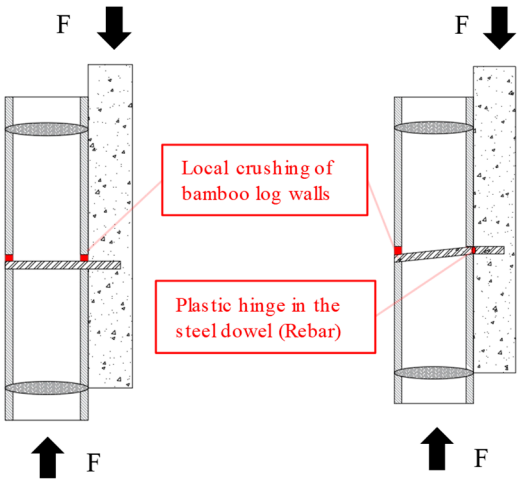


**Figure 6.** Possible modes of failures in bamboo-concrete dowel-type shear connections.

(a) "Pure" embedment strength in bamboo.

(b) Embedment strength in bamboo combined with the formation of one plastic hinge in the dowel at the interface.

The idealized failure modes are illustrated in Figure 6. This approach is based on the tubular nature of bamboo (as opposed to massive timber) and on the assumption of a strong and stiff embedment in concrete, consistent with the approach proposed in [28] for steel-to-timber connections using a thick steel plate [33]. The corresponding predictive equations for the identified failure modes are presented in Table 4.

**Table 4.** Predictive design equations for dowel-type shear connections in bamboo-concrete composite solutions.

| Failure Mode | Proposed Equation | |
|---|---|---|
| mode (a) | $F_{R,a} = f_{h,B}(2t_B)d_R$ | (8) |
| mode (b) | $F_{R,b} = f_{h,B}(2t_B)d_R\left[\sqrt{2+\frac{4M_{y,R}}{f_{h,B}d_R(2t_B)^2}}-1\right]$ | (9) |
| Dowel-type shear connection | Min ($F_{R,a}$; $F_{R,b}$) | (10) |

2.3.3. Notch and Dowel Connection (SND)

When both notch and dowel mechanisms are used to achieve shear transfer between the two materials, as illustrated in Table 1, the load is expected to be shared between the two connection systems. This combined behavior was observed in the experimental tests discussed in Section 3.2. The global load-transfer mechanism can therefore be represented by a parallel system of springs, in which the proportion of load carried by each component is governed by its stiffness. If the stiffer component exhibits sufficient deformation capacity, the total load-carrying capacity of the connection can be considered as the sum of the individual strengths, as expressed in Equation (11). Conversely, if the stiffer component, such as the concrete notch connection, shows limited deformation at maximum load, the load transfer through the dowel mechanism must be restricted according to the compatibility of deformations, i.e., the maximum deformation of the notch connection, as expressed

in Equation (12). The latter case assumes a linear load–deformation response up to the ultimate capacity of the notch connection.

$$F_{v,R} = F_{v,N} + F_{v,D} \tag{11}$$

$$F_{v,R} = F_{v,N} + k_{slip,D}\frac{F_{v,N}}{k_{slip,N}} \tag{12}$$

where: $F_{v,N}$ is the load capacity of notch connection computed as described in Section 2.3.1; $F_{v,D}$ is the load capacity of the dowel connection as described in Section 2.3.2; $K_{slip,D}$ is the slip modulus of the dowel connection (at this stage taken from tests); $K_{slip,N}$ is the slip modulus of the notch connection taken from tests.

## 3. Results

### *3.1. Material Tests*

Compression tests on concrete cubes (150 mm$^3$) were performed after 28 days of curing, in accordance with EN 12390-3 [34]. The resulting compressive strength values are presented in Table 5. The compressive strength of bamboo parallel to the grain was also determined following ISO 22157 [35], using a total of 11 specimens. As cracks in bamboo culms are unavoidable, both cracked and uncracked samples were tested. As shown in Table 5, the presence of cracks did not significantly affect the compressive strength, as both sample types exhibited comparable values. The average moisture content of the bamboo at the time of testing was 11.8%.

**Table 5.** Materials compressive strength (N/mm$^2$).

| Concrete (28 days) | Bamboo (Cracked) | Bamboo (Uncracked) | Bamboo (All) |
|---|---|---|---|
| 40.2<br>σ = 4.2<br>COV = 10.4% | 62.8<br>σ = 2.8<br>COV = 4.4% | 66.5<br>σ = 5.0<br>COV = 7.6% | 64.5<br>σ = 4.4<br>COV = 6.8% |

### *3.2. Push-Out Tests*

The mechanical behavior of the tested connections was evaluated through force–deformation and force–slip curves. The force–deformation curve represents the overall displacement between the load application point and the reaction support. In contrast, the force–slip curve excludes the axial deformation of the materials, thereby isolating the relative slip caused by connection deformation.

The following sub-sections present the response of each test series, followed by a summary of the key mechanical properties, including: (i) the initial connection stiffness ($k_{slip}$), calculated according to ISO 6891 [36] and EN 26891 [26] and defined in Equation (13); (ii) the maximum load capacity ($F_{max}$); (iii) the slip corresponding to the maximum load ($\delta_{F_{max}}$); and (iv) the ultimate slip ($\delta_u$), defined as the slip corresponding to 80% of $F_{max}$ in the post-peak range. Finally, the failure modes governing the load capacity of each test series are presented.

$$k_{slip} = \frac{0.3F_{max}}{(\delta_{0.4} - \delta_{0.1})} \tag{13}$$

where: $\delta_{0.4}$ and $\delta_{0.1}$ are the slip of the connection at load corresponding to 40% and 10% of the load capacity (Fmax), respectively.

#### 3.2.1. Short Notch (SN) Shear Connection

In Figure 7, the force–deformation (dashed line) and force–slip (continuous line) curves exhibit minimal differences, indicating that the axial deformations of the concrete layer and

bamboo log are negligible. The three replicates display similar initial load–slip responses; however, within the ascending branch, the curves begin to diverge. This divergence can be attributed to pre-existing cracks in some bamboo logs, as previously noted. Specimen SN-1, which showed no visible cracking, exhibited a smoother load–slip response. Although cracking affected some specimens more than others, their overall load capacities remained within a comparable range. Beyond the peak load, the specimens exhibited a brittle post-peak response, characterized by a sharp loss of load-carrying capacity.

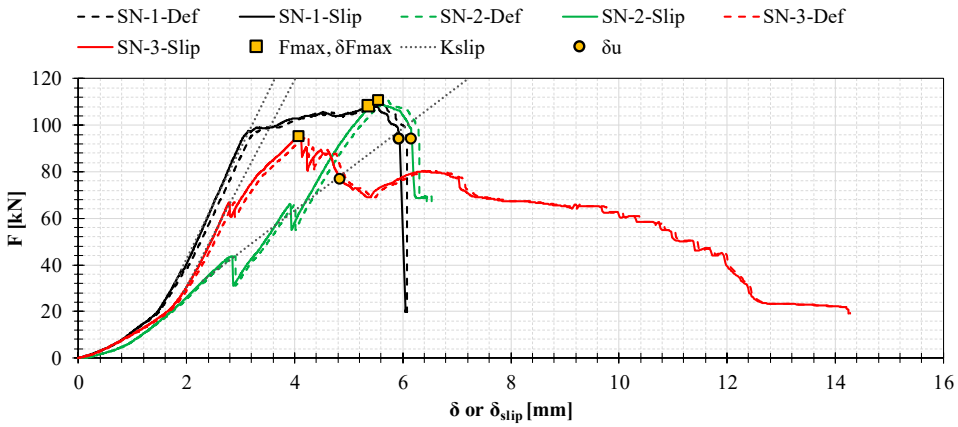


**Figure 7.** Force-deformation and force-clip curves of SN test specimens.

### 3.2.2. Long Notch (LN) Shear Connection

In this series, only two specimens were tested due to significant imperfections in one sample, which led to excessive loading eccentricity. As shown in Figure 8, the difference between the overall specimen deformation and the connection slip was again negligible. Similar to the previous configuration, variability in specimen stiffness is evident and may be attributed to local cracking. Despite this, the values of maximum load remain within the same order. Although the limited number of specimens prevents drawing broad conclusions, the post-peak response appears smoother, with a more gradual loss of load-carrying capacity.

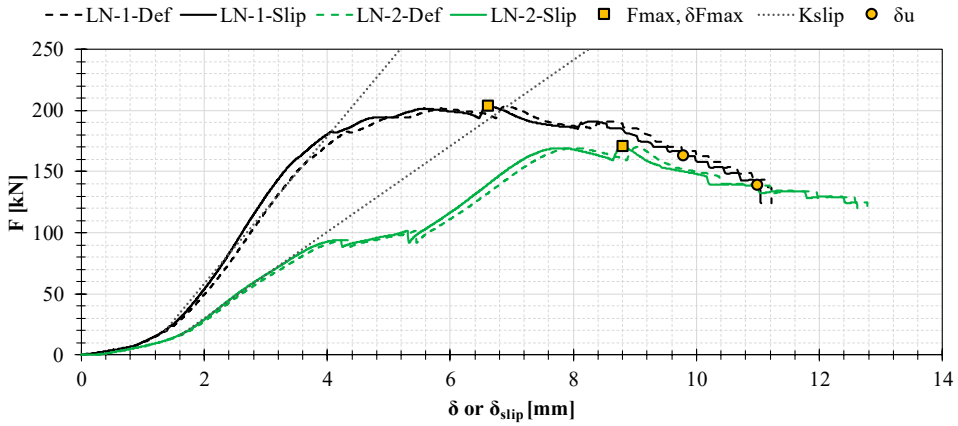


**Figure 8.** Force-deformation and force-clip curves of LN test specimens.

### 3.2.3. Dowel (D) Shear Connection

In this series, no difference was observed between the deformation and slip responses, as the corresponding curves nearly overlapped (Figure 9). This behavior is attributed to the low load capacity of the connection, which results in negligible deformation of the specimen components. The reduced load capacity reflects a distinct load transfer mechanism—dowel action in both the concrete and bamboo. The limited contact area, combined with the

low bending stiffness of the dowel, promotes local crushing of the bamboo around the dowel (hole elongation) and plastic deformation of the dowel itself. Moreover, this type of connection exhibits the ability to deform without a significant loss of load, a behavior commonly reported in studies involving similar load transfer mechanisms [16]. Although some variability is observed in the ascending branch, the load capacities of the specimens remain comparable.

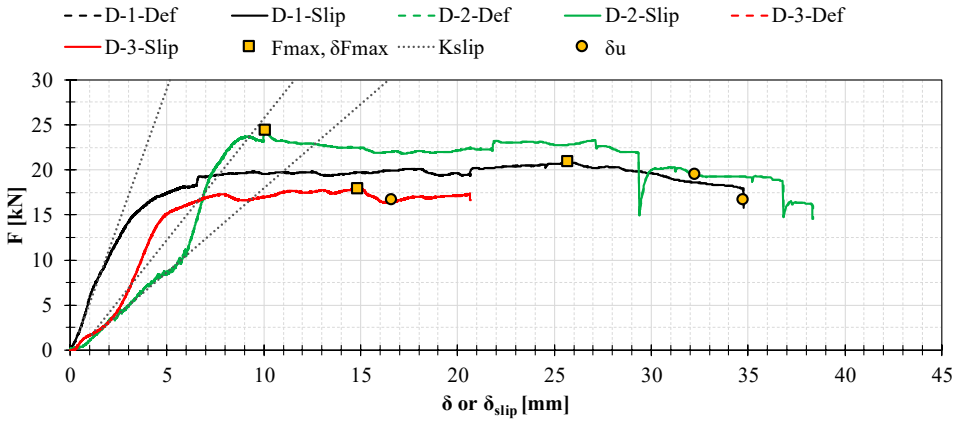


**Figure 9.** Force-deformation and force-clip curves of D test specimens.

### 3.2.4. Combined Short Notch and Dowel (SND) Shear Connection

The connection behavior illustrated in Figure 10 exhibits a more stable response. The combined load transfer mechanism, dowel action coupled with mechanical interlock through the notch, appears to mitigate the sensitivity of the connection to defects in the joined components. Although this configuration does not display the same deformation capacity as the pure dowel connection, the addition of the dowel significantly enhances the brittle response of the notched connection when used alone.

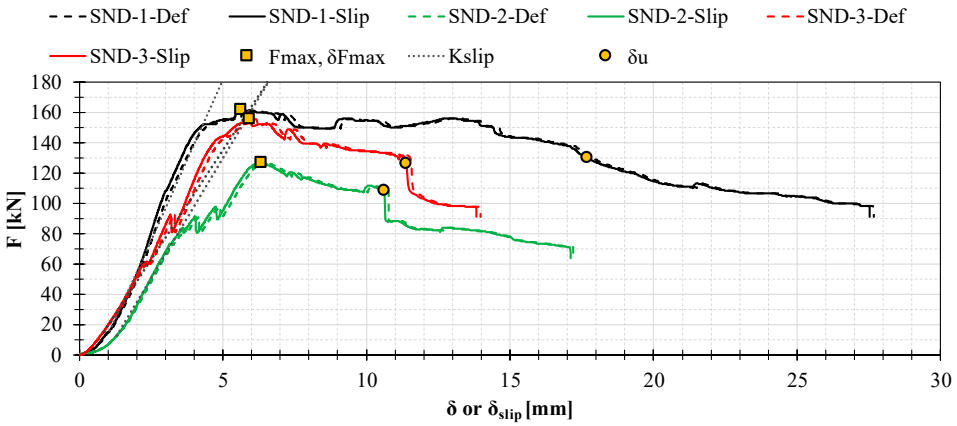


**Figure 10.** Force-deformation and force-clip curves of SND test specimens.

### 3.2.5. Failure Modes and Overview of the Main Mechanical Properties

The distinct mechanical responses observed among the investigated shear connection configurations are reflected in the corresponding failure modes governing the maximum load achieved during testing. The failure modes identified for each configuration are summarized below and illustrated in Figure 11.


**Figure 11.** Observed failure modes in the 4 tested shear connection configurations. (**a**) Test series SN. (**b**) Test series LN. (**c**) Test series D. (**d**) Test series SND.

- **Test series SN:** Shear failure of the concrete at the bamboo–concrete interface (Figure 11a).
- **Test series LN:** Bamboo crushing under compression (Figure 11b).
- **Test series D:** Dowel–bamboo embedment deformation characterized by local bamboo crushing and elongation of the dowel hole, accompanied by dowel plastic deformation (Figure 11c).
- **Test series SND:** Combined shear failure of the concrete at the bamboo–concrete interface and dowel–bamboo embedment deformation (Figure 11d).

To provide an overall summary of the mechanical performance of the investigated bamboo–concrete shear connections, Table 6 presents the key mechanical parameters discussed above. These have been also identified in the load-slip curves presented in the presented in Sections 3.2.1–3.2.4. Note that for SN series, the connection stiffness has been computed between 30% and 60% of $F_{max}$ in order to eliminate the initial system slip still noticeable in the force-slip curves above 10% $F_{max}$. Given the limited number of tested specimens and the presence of imperfections inherent to both the materials (e.g., the natural variability of bamboo) and the experimental procedures (as previously mentioned, the concrete casting layout and the resulting inadequate vibration), the statistical significance of the results must be interpreted with caution. Despite these limitations, the findings provide valuable preliminary insights into the mechanical behavior of the various connection types. A more detailed comparison of the influencing variables is presented in the following chapter.

- **Connection stiffness:** The dowel-type connection exhibited the lowest stiffness among the tested configurations, whereas the long-notch connection was the stiffest. This parameter also showed the highest coefficient of variation across all series, reflecting the influence of cracking observed in the load–slip response.
- **Maximum force:** Consistent with the stiffness trends, the dowel-type and long-notch connections displayed the lowest and highest load capacities, respectively. In contrast to stiffness, the load capacity generally exhibited lower variability, corroborating the observations made in the load–slip behavior discussion.
- **Deformation at maximum force:** As expected, the dowel-type connection reached its maximum load at higher slip values due to its lower stiffness, while the other configurations attained peak load at comparable slip levels.
- **Ultimate deformation:** The results clearly indicate that the inclusion of a dowel, whether used alone or in combination with a notch, enhances ductility. Although these configurations showed higher coefficients of variation, the increase in ultimate deformation is significant, confirming an effective improvement in ductile behavior.

**Table 6.** Summary of the key mechanical properties of the tested connections.

| Test Series | $K_{slip}$ [kN/mm] | $F_{max}$ [kN] | $\delta_{Fmax}$ [mm] | $\delta_u$ [mm] |
|---|---|---|---|---|
| SN-i | 47.3; 17.7; 44.0 | 108.1; 110.8; 95.1 | 5.4; 5.6; 4.1 | 5.9; 6.2; 4.8 |
| | μ = 36.3<br>σ = 13.3<br>COV = 36.5% | μ = 104.7<br>σ = 6.8<br>COV = 6.5% | μ = 5.0<br>σ = 0.7<br>COV = 13.0% | μ = 5.7<br>σ = 0.6<br>COV = 10.2% |
| LN-i | 60.0; 35.14 | 203.6; 170.2 | 6.6; 8.8 | 9.8; 11.0 |
| | μ = 47.6<br>σ = 12.4<br>COV = 26.1% | μ = 186.9<br>σ = 16.7<br>COV = 8.9% | μ = 7.7<br>σ = 1.1<br>COV = 14.1% | μ = 10.4<br>σ = 0.6<br>COV = 5.8% |
| D-i | 5.9; 1.9; 2.7 | 20.8; 24.3; 17.9 | 25.7; 10.1; 14.9 | 34.7; 32.3; 16.6 |
| | μ = 3.5<br>σ = 1.8<br>COV = 50.3% | μ = 21.0<br>σ = 2.6<br>COV = 12.5% | μ = 16.9<br>σ = 6.5<br>COV = 38.7% | μ = 27.9<br>σ = 8.0<br>COV = 28.8% |
| SND-i | 42.0; 31.7; 28.8 | 161.6; 126.8; 155.8 | 5.6; 6.4; 5.9 | 17.7; 10.6; 11.4 |
| | μ = 34.2<br>σ = 5.7<br>COV = 16.6% | μ = 148.1<br>σ = 15.2<br>COV = 10.3% | μ = 6.0<br>σ = 0.3<br>COV = 4.8% | μ = 13.2<br>σ = 3.2<br>COV = 24.0% |

## 4. Discussion

### *4.1. Comparison Between Investigated Connections*

To complement the comparison of the mechanical performance of the investigated shear connections, Figure 12 presents, for each mechanical property, the ratio between the value obtained for each specimen and the overall mean value ($\mu_{all}$) of the corresponding property. The ratio between the meaning of each test series and the overall mean is also included (red cross points).

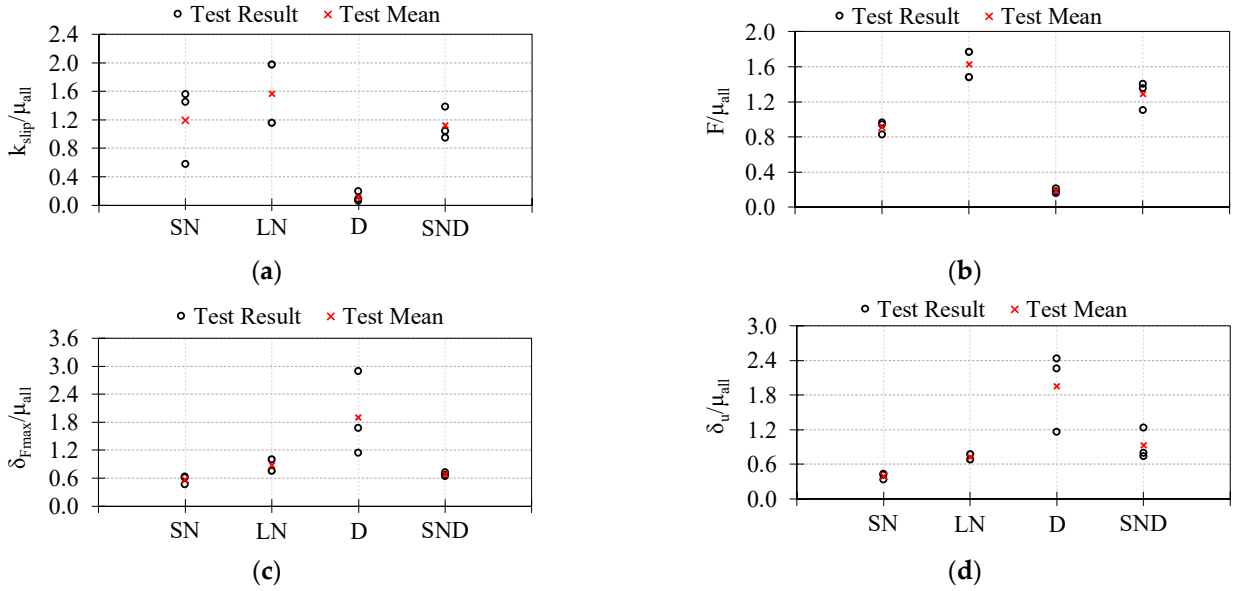


**Figure 12.** Comparison of mechanical properties of the tested specimens. (**a**) Stiffness ($k_{slip}$). (**b**) Load capacity ($F_{max}$). (**c**) Deformation at $F_{max}$ ($\delta_{Fmax}$). (**d**) Deformation at $F_{max}$ ($\delta_u$).

The long-notch (LN) connection outperformed all other configurations in terms of both stiffness and load capacity. According to the computed ratios, the LN connection exhibited approximately 1.3 and 1.8 times, respectively, the stiffness and resistance of the small-

notch (SN) connection. In contrast, the dowel-type (D) connection showed the weakest performance, suggesting that the composite action between bamboo and concrete would be significantly limited. When compared with the LN configuration, the D connection exhibited approximately eight times lower stiffness and strength.

The combination of dowel and notch mechanisms (SND) resulted in an added mechanical contribution. Figure 13 compares the sum of the mean values from series D and SN with the corresponding mean values from series SND for both connection stiffness and load capacity. The combined system outperformed the sum of the individual systems in terms of load capacity, showing an increase of approximately 18%. In contrast, a decrease of 5.9% was observed for connection stiffness. Although an improvement might be expected given the additive nature of the mechanisms, the substantial difference between the stiffness values of the individual systems (with SN being dominant), together with the variability observed in the tests, justifies the slight reduction recorded. Nonetheless, the key observation is that, in terms of strength, a synergistic effect was achieved.

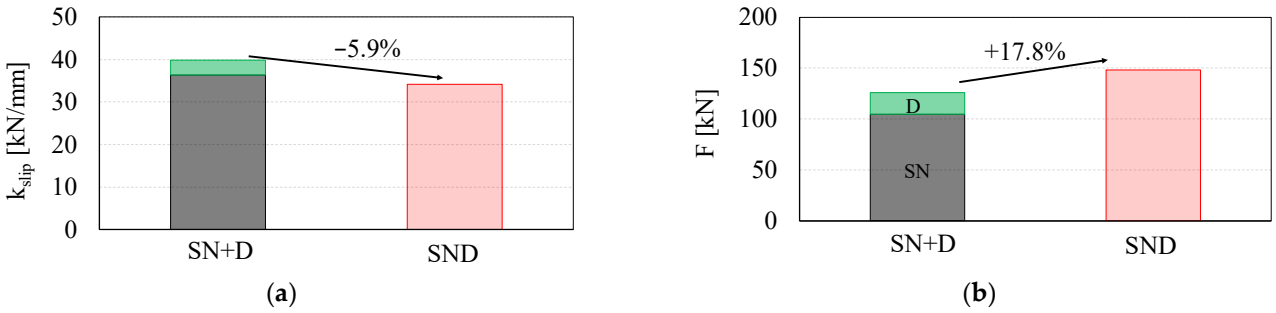


**Figure 13.** Quantification of the added contribution of dowel and notch connection system. (**a**) Stiffness ($k_{slip}$). (**b**) Load capacity ($F_{max}$).

In terms of deformability, Figure 12 further highlights the significant contribution of the dowel, which, in the SND configuration, mitigates the brittle response typical of a notch-only connection. This represents a major advantage of the combined system: it not only delivers superior performance under service load conditions (enhanced composite action and bending stiffness) but also provides notable deformation capacity, contributing to a more ductile behavior at the ultimate limit state.

### *4.2. Assessment of Predictive Models*

The comparison between the proposed predictive models and the experimental results is presented in Table 7. Based on this comparison, the following observations can be made:

- **SN:** The analytical model predicts a relatively low shear resistance for the bamboo (61.8 kN). This estimate assumes the bamboo is free of knots and that all load transfer occurs through the mechanical interlock along the bamboo wall thickness. However, in this configuration, the concrete penetrates and fills the interior of the bamboo culm, enabling an additional load transfer mechanism through the knot–concrete interface. Consequently, limiting the connection's load capacity only to the shear planes represented in Figure 5c is overly conservative, as confirmed by the test results. A more accurate determination of the load capacity for this mode would require quantifying the contact area between the internal concrete core and the knots, which was beyond the scope of the present experimental program. Since shear failure of the bamboo log was not observed during testing, this failure mode can be disregarded. The subsequent failure mode predicted by the analytical model, shear of concrete, is consistent with experimental observations, indicating reasonable agreement in the predicted behavior. Regarding accuracy, the analytical model slightly overestimates the measured

strength. The deviations can be attributed to: (i) the concrete quality, as inadequate vibration may have caused internal voids or heterogeneity, promoting early cracking; and, (ii) geometric imperfections in the specimens, resulting in deviations between the actual and idealized shear plane dimensions assumed in the model.

- **LN:** The predicted failure mode, crushing of bamboo, matches the experimental observations. The estimated load capacity provides a reasonable approximation and does not exceed the mean experimental strength, indicating a conservative and safe prediction. It is worth noting that, similar to the bamboo shear model, the analytical formulation simplifies the interaction by considering only the contact area within the notch zone (see Figure 5d). In reality, due to the presence of concrete inside the bamboo, some load redistribution is expected beyond this localized area. Therefore, assuming a limited contact zone defined by the wall thickness and notch arc length is conservative. As shown in Figure 11b, bamboo crushing occurs primarily at the bottom portion of the log, in an area corresponding approximately to the notch contact zone. This suggests that compressive stresses are concentrated in a region proportional to that assumed in the model. Hence, the proposed analytical approach can be considered consistent, providing a safe yet not overly conservative prediction.
- **D:** For this connection type, both the predicted failure modes and the load capacities are in close agreement with the experimental results, indicating that the analytical model is appropriate for this configuration.
- **SND:** The predicted failure modes and load capacities show satisfactory agreement for this configuration. Although the results may be influenced by material and geometric imperfections in the specimens, as previously discussed, the combined contribution of both connection systems appears to be an appropriate design approach. Moreover, Equation (12) demonstrates very good accuracy, indicating that the dowel's contribution should be evaluated based on the compatibility of deformations within the connection, since the notch mechanism does not exhibit sufficient deformation capacity to achieve the full plastic resistance of dowel-type system.

**Table 7.** Comparison of results between predictive models and experimental tests.

| Configuration | Analytical Prediction | | Test | |
|---|---|---|---|---|
| | **F [kN]** | **Mode of Failure** | | **F [kN]** |
| SN | 135.2 | (a) (assuming cracked concrete) | 104.7 | Shear of concrete |
| LN | 170.7 | Bamboo crushing | 187.0 | Bamboo crushing |
| D | 22.6 | 1 Plastic hinge | 21.0 | 1 Plastic hinge |
| SND | 157.7 (Equation (11))<br>148.2 (Equation (12)) | (a) + Plastic hinge | 148.7 | (a) + Plastic hinge |

## 5. Conclusions

In this study, three connection methods were investigated to achieve an efficient shear connection between bamboo logs and a concrete layer, thereby enabling composite action. The analyzed configurations included: (i) a notch-type connection, (ii) a dowel-type connection, and (iii) a combined notch–dowel system. Such solutions have not previously been explored at the connection level (isolated) to better understand the efficiency of possible connections solutions.

The mechanical behavior of these connection systems was characterized through experimental testing, and analytical models were proposed to predict their load-bearing capacity. The main findings are summarized as follows:

(1) Notch-type vs. dowel-type behavior: The notch-type connection exhibited higher strength and stiffness, but failed in a brittle manner. In contrast, the dowel-type connection showed lower strength (D/SN $\approx$ 0.2 and D/LN $\approx$ 0.1) and stiffness (D/SN $\approx$ 0.10 and D/LN $\approx$ 0.07) but demonstrated significant plastic deformation capacity (D/SN $\approx$ 4.9 and D/LN $\approx$ 2.7), resulting in a more ductile response.

(2) Influence of notch geometry: Increasing the notch length in the bamboo log improved strength (LN/SN $\approx$ 1.8), stiffness (LN/SN $\approx$ 1.3), and deformation capacity (LN/SN $\approx$ 1.8). Experimental observations revealed that specimens with shorter notches failed primarily due to concrete in shear, while those with longer notches failed by bamboo crushing.

(3) Combined notch–dowel connection (SND): The combination of a shorter notch with a dowel showed a clear synergistic effect for resistance, as reflected in the experimental results. This configuration provided a well-balanced solution. Compared to short-notch connections (SN), the combined system exhibited equivalent stiffness (SND/SN $\approx$ 0.94) and improved strength (SND/SN $\approx$ 1.4), falling between the short and long notch values, and achieved more than double (SND/SN $\approx$ 2.3) the deformation capacity ($\delta_u$) without a significant loss of strength.

(4) Sources of variability: The variability observed in the experimental results reflects several challenges inherent to testing natural materials and composite systems: (i) the limited number of specimens (three per configuration) due to the scope of the study; (ii) natural imperfections in bamboo, such as variations in diameter, presence of knots, and surface cracks; and (iii) execution-related imperfections, including variations in notch cutting, bamboo placement, concrete infill quality, and vibration effectiveness.

(5) Analytical model performance: The proposed predictive models successfully captured the main mechanical behavior of the different connection systems. For each configuration, the relevant failure modes were identified and corresponding analytical expressions proposed. Despite the challenges in accurately evaluating certain modes, particularly those influenced by the concrete infill, the comparison between analytical and experimental results demonstrated satisfactory agreement. The governing failure modes were consistently predicted, and the load-carrying capacity estimates were acceptable given the limited sample size and material variability.

Overall, despite the inherent limitations of the experimental program, the study successfully characterized the mechanical behavior of the four investigated shear connection types and provided a qualitative understanding of their performance. Among the tested configurations, the combined short-notch and dowel system (SND) is recommended as the most balanced solution, offering an effective compromise between stiffness, strength, and ductility; thus enabling efficient bamboo–concrete composite action. Moreover, adopting shorter notches (SN) can reduce weakening of the bamboo log under bending compared to longer notches (LN). However, this assumption should be further validated through bending tests on full-scale composite elements.

Finally, although the main objective of this research, critically evaluating different connection solutions for the development of high-performance bamboo–concrete composite members (e.g., beam floors), has been achieved, several limitations were identified that should be addressed in future studies. Specifically: (i) the geometrical variability of bamboo logs should be reduced through a preliminary grading process in which defects and dimensional variations are classified within available batches, potentially using non-destructive testing techniques; (ii) the concrete casting procedure should be modified

or improved to ensure better vibration, reduce material heterogeneity and guaranty full concrete infill; (iii) now that the most promising configuration has been identified, the number of variants studied can be reduced, allowing an increase in the number of replicates and, consequently, greater statistical significance; and (iv) conduct specific tests to evaluate the strength of the knot area when full concrete infill is obtained. Implementing these measures would help mitigate the variability observed in the reported experiments and support the further validation and eventual improvement of the proposed analytical models. However, it must be recognized that bamboo is a natural material, and for the proposed composite solution, complete control of its variability remains limited. Next, since the intended application of the system is in flooring, subsequent research should include bending tests to more realistically assess its structural performance. Furthermore, while the immediate focus is on understanding the short-term mechanical efficiency of the system (an essential and cost-effective first step), time-dependent behavior, durability, and life-cycle performance, must also be investigated to fully validate the proposed solution for practical use.

**Author Contributions:** Conceptualization, J.H. and J.J.; methodology, J.H.; formal analysis, J.H.; investigation, J.H. and J.J.; resources, J.H. and J.J.; writing—original draft preparation, J.H.; writing—review and editing, J.H. and J.J.; supervision, J.H.; project administration, J.H. and J.J.; funding acquisition, J.H. and J.J. All authors have read and agreed to the published version of the manuscript.

**Funding:** This research was funded by Belgian federal government (Directorate-General for Development Cooperation and Humanitarian Aid (DGD)) through the project "ASSURE—A Sustainable Construction for Ethiopia: Integrating Local, Resources for Affordable, Resilient and Sustainable Housing", a short initiative project (ET2023SIN384A104) financed by the general financial framework for VLIR-UOS-funded projects of the Five-Year Programme 2022–2027 (FYP2).

**Data Availability Statement:** The data presented in this study are available on request from the corresponding author. The data are not publicly available due to privacy.

**Acknowledgments:** The authors express their sincere gratitude to the following for their help in the execution of the experimental work: Hasselt University students (academic year 2023–2024) Thomas Swennen, Senne Vranken, Warre Wels; Jimma University student (academic year 2023–2024) Kaleb Bekele Ossu; and the personal of the Applicatie Centrum Beton en Bouw of the Construction Engineering Research Group of Hasselt University.

**Conflicts of Interest:** The authors declare no conflicts of interest.

## References

1. Hradil, P.; Fülöp, L.; Vares, S.; Wahlström, M.; Rantala, J.; Kilpi, L.; Mäkeläinen, T.; Tiihonen, N.; Sansom, M.; Pimentel, R.; et al. Provisions for a Greater Reuse of Steel Structures. In *PROGRESS, Final Report*; European Commission, Research Fund for Coal and Steel, Grant Agreement number: 747847—PROGRESS—RFCS-2016/RFCS-2016. 2020. Available online: https://www.steelconstruct.com/wp-content/uploads/PROGRESS-final-report-for-web.pdf?utm_source=chatgpt.com (accessed on 18 November 2025).
2. United Nations. *The World's Cities in 2018—Data Booklet*; Department of Economic and Social Affairs, Population Division. 2018. Available online: https://www.un.org/en/development/desa/population/publications/pdf/urbanization/the_worlds_cities_in_2018_data_booklet.pdf?utm_source=chatgpt.com (accessed on 18 November 2025).
3. Raye, G.; Getachew, S.; Gizaw, M.; Kaba, M. Vulnerability to housing and the environment in urban settings: Implications for residents and places. *Ethiop. J. Health Dev.* **2020**, *34*, 24–32.
4. Yadav, M.; Mathur, A. Bamboo as a sustainable material in the construction industry: An overview. *Mater. Today Proc.* **2021**, *43*, 2872–2876. [CrossRef]
5. Fahim, M.; Hais, M.; Khan, W.; Zaman, S. Bamboo as a Construction Material: Prospects and Challenges. *Adv. Sci. Technol. Res. J.* **2022**, *16*, 165–175. [CrossRef] [PubMed]
6. Xiao, Y.; Inoue, M.; Paudel, S.K. Modern bamboo structures. In Proceedings of the First International Conference on Modern Bamboo Structures, ICBS-2007, Changsha, China, 28–30 October 2007.

7. Zhao, Y.; Feng, D.; Jayaraman, D.; Belay, D.; Sebrala, H.; Ngugi, J.; Maina, E.; Akombo, R.; Otuoma, J.; Mutyaba, J.; et al. Bamboo mapping of Ethiopia, Kenya and Uganda for the year 2016 using multi-temporal Landsat imagery. *Int. J. Appl. Earth Obs. Geoinf.* **2018**, *66*, 116–125. [CrossRef]
8. Bahru, T.; Ding, Y. A Review on Bamboo Resource in the African Region: A Call for Special Focus and Action. *Int. J. For. Res.* **2021**, *2021*, 8835673. [CrossRef]
9. Ahmad, J.; Zhou, Z.; Deifalla, A.F. Structural properties of concrete reinforced with bamboo fibers: A review. *J. Mater. Res. Technol.* **2023**, *24*, 844–865. [CrossRef]
10. Moshiri, F.; Gerber, C.; Crews, K. State of the art on Timber Concrete Composite floor. In Proceedings of the 25th Biennial Conference of Concrete Institute of Australia, Perth, Australia, 12–14 October 2011.
11. COST. Design of timber-concrete composite structures—A state-of-the-art. In *Report by COST Action FP1402/WG 4*; Shaker Verlag: Aachen, Germany, 2018.
12. Ghavami, K. Bamboo as reinforcement in structural concrete elements. *Cem. Concr. Compos.* **2005**, *27*, 637–649. [CrossRef]
13. Govindan, B.; Ramaamy, V.; Pannerselvam, B.; Rajan, D. Performance assessment on bamboo reinforced concrete beams. *Innov. Infrastruct. Solut.* **2022**, *7*, 16. [CrossRef]
14. Akmaluddin; Pathurahman; Suparjo; Gazalba, Z. Flexural behavior of steel reinforced lightweight concrete slab with bamboo permanent formworks. *Procedia Eng.* **2015**, *125*, 865–872. [CrossRef]
15. Martins, C.; Dias, A.; Costa, R. Reinforcement of timber floors using lightweight concrete—Mechanical behaviour of connections. In Proceedings of the COST Action FP 1004—Experimental Research with Timber, Prague, Czech Republic, 21–24 May 2014.
16. Appavuravther, E.; Vandoren, B.; Henriques, J. Behaviour of bonded-in dowel shear connections in timber lightweight concrete composite beams including effect of an interlayer. *Constr. Build. Mater.* **2023**, *397*, 132389. [CrossRef]
17. Rasmussen, P.K.; Sørensen, J.H.; Hoang, L.C.; Feddersen, B.; Larsen, F. Notched connection in timber-concrete composite deck structures: A literature review on push-off experiments & design approaches. *Constr. Build. Mater.* **2023**, *397*, 131761. [CrossRef]
18. *CEN/TS 19103*; Eurocode 5: Design of Timber Structures—Structural design of Timber-Concrete Composite Structures—Common Rules and Rules for Buildings. European Committee for Standardization: Brussels, Belgium, 2021.
19. Oehlers, D.J.; Nguyen, N.T.; Ahmed, M.; Bradford, M.A. Partial Interaction in Composite Steel and Concrete Beams with Full Shear Connection. *J. Constr. Steel Res.* **1997**, *41*, 235–248. [CrossRef]
20. Dias, A.M.P.G.; Jorge, L.F.C. The effect of ductile connectors on the behaviour of timber–concrete composite beams. *Eng. Struct.* **2011**, *33*, 3033–3042. [CrossRef]
21. Lukaszewska, E.; Fragiacomo, F.; Frangi, A. Evaluation of the slip modulus for ultimate limit state verifications of timber-concrete composite structures. In Proceedings of the CIB-W18, International Council for Research and Innovation in Building and Construction-Working Commission W18-Timber Structures, Bled, Slovenia, 27–30 August 2007.
22. Gutkowski, R.; Brown, K.; Shigidi, A.; Natterer, J. Investigation of notched composite wood-concrete connections. *J. Struct. Eng. (ASCE)* **2004**, *130*, 1553–1561. [CrossRef]
23. Dias, A. Mechanical Behaviour of Timber-Concrete Joints. Ph.D. Thesis, TU Delft, Delft, The Netherlands, 4 April 2005.
24. Dias, A.M.P.G.; Kuhlmann, U.; Kudla, K.; Mönch, S.; Dias, A.M.A. Performance of dowel-type fasteners and notches for hybrid timber structures. *Eng. Struct.* **2018**, *171*, 40–46. [CrossRef]
25. Appavuravther, E.; Martins, C.; Vandoren, B.; Dias, A.; Henriques, J. Efficiency of timber-concrete composite floors with discrete perfobond connections: A numerical study. *Eng. Struct.* **2024**, *303*, 117511. [CrossRef]
26. *EN 26891*; Timber Structures—Joints Made with Mechanical Fasteners—General Principles for the Determination of Strength and Deformation Characteristics. CEN, European Committee for Standardization: Brussels, Belgium, 1991.
27. *EN 1994-1-1*; Eurocode 4: Design of Composite Steel and Concrete Structures—Part 1-1: General Rules and Rules for Buildings. CEN, European Committee for Standardization: Brussels, Belgium, 2004.
28. *EN 1995-2*; Eurocode 5: Design of Timber Structures—Part 2: Bridges. European Committee for Standardization: Brussels, Belgium, 2004.
29. *EN 1992-1-1*; Eurocode 2: Design of Concrete Structures—Part 1-1: General Rules and Rules for Buildings. European Committee for Standardization: Brussels, Belgium, 2004.
30. Pujol, S.; Hanai, N.; Ichinose, T.; Sozen, M.A. Using Mohr-Coulomb Criterion to Estimate Shear Strength of RC Columns. *ACI Struct. J.* **2016**, *113*, 459–468. [CrossRef]
31. Johansen, K. Theory of timber connections. *Int. Assoc. Bridge Struct. Eng.* **1949**, *9*, 249–262.
32. Meyer, A. Die Tragfähigkeit von Nagelverbindungen bei statischer Belastung. *Holz Als Roh-Und Werkst.* **1957**, *15*, 96–109. [CrossRef]
33. *EN 1995-1-1*; Eurocode 5: Design of Timber Structures—Part 1-1: General Rules and Rules for Buildings. European Committee for Standardization: Brussels, Belgium, 2004.
34. *EN 12390-3*; Testing Hardened Concrete—Part 3: Compressive Strength of Test Specimens. CEN, European Committee for Standardization: Brussels, Belgium, 2019.

35. *ISO 22157*; Bamboo Structures—Determination of Physical and Mechanical Properties of Bamboo Culms—Test Methods. ISO: Geneva, Switzerland, 2019.
36. *ISO 6891*; Timber Structures—Joints Made with Mechanical Fasteners—General Principles for the Determination of Strength and Deformation Characteristics. ISO: Geneva, Switzerland, 1983.